Horizontal Load Implementation Techniques Using Asphalt Pavement Computer Program Apbi

Yipeng Chen[1,2,3], Xin Jiang[1,2,3,*], Yangchen Lu[1,2,3], Xinya Huang[1,2,3], Canyang Cui[1,2,3], Yang Xue[1,2,3], Shixuan Li[1,2,3], Hongpo Liu[1,2,3] and Yanjun Qiu[4]

[1]*School of Smart City and Transportation, Southwest Jiaotong University, Chengdu 610031, China*

[2]*Highway Engineering Key Laboratory of Sichuan Province, Southwest Jiaotong University, Chengdu 610031, China*

[3]*MOE Key Laboratory of High-speed Railway Engineering, Southwest Jiaotong University, Chengdu 610031, China*

[4]*School of Civil Engineering, Tarim Institute of Technology, Alaer 843399, China*

Abstract: The computer program Apbi, developed based on elastic layered system theory, is applicable to the analysis of layered elastic systems including multilayer flexible pavements, airport pavements, and multilayer foundations, and has been widely adopted in academic research and engineering practice. However, its full source code has not been publicly released, and a complete official user manual is currently unavailable. When one or more horizontal loads are applied, the input specification of Apbi is not clearly defined. In addition, the computational accuracy and reliability of its stress predictions under such loading conditions have not been systematically verified. To fill these research gaps, this study designs a variety of load combination scenarios to clarify Apbi's input specifications under different horizontal load conditions. The stress outputs from Apbi are validated against calculation results from the well-recognized GAMES program. Moreover, a practical approximate calculation method is proposed for working conditions subjected purely to horizontal loads. This study also identifies that Apbi yields incorrect values for the two in-plane shear stress components inside the loaded area on the pavement surface, which offers a practical reference for the proper application of the Apbi program in the design and calculation of multilayer flexible pavements, airport pavements, and multilayer foundations.

Keywords: Apbi, horizontal load, input format, reliability evaluation, calculation error.

1. INTRODUCTION

Asphalt pavements possess distinct horizontal layered features. Accurate acquisition of pavement structural mechanical responses including stress, strain and displacement under load is directly related to the scientific validity, service safety, and durability of pavement structural design, and is of great significance for pavement design implementation and the elucidation of damage mechanisms [1]. To efficiently and accurately calculate the mechanical behavior of elastic layered systems under applied loads, multiple computational programs have been developed. Typical representatives include the U.S.-developed KENLAYER [2-5], ELSYM5 [6], Everstress [7], WinJULEA [8] and WESLEA [9]; the Netherlands-developed BISAR [10]; as well as Japan-developed GAMES [11].

China has also developed several computer programs, including NESCP and Apbi. The Apbi program claims the ability to address various complex loading conditions, such as multiple wheel loads, multi-layered structures, imperfect interlayer contact, and horizontal loads [12]. In addition to its application in mechanical analysis of asphalt pavements, the Apbi program can also be adopted to calculate stress and deformation of multilayer foundations, for instance, solving problems regarding the determination of the subgrade work zone. This program has garnered widespread attention from academia and engineering communities focusing on asphalt pavement research in recent years. Representative studies are as follows: Chen and Huang calculated the stress distribution in each pavement layer under heavy loading by using temperature-dependent material moduli, and analyzed the effects of load, temperature, and horizontal braking force on the stress state [13]; Huang and Gao computed the surface deflection and tensile stress at the bottom of the semi-rigid base under different axle loads, developed an axle load equivalence exponent based on elastic layered system theory, and compared it with nonlinear finite element results to demonstrate the limited applicability of the current specification's axle load equivalence formula under heavy loading conditions [14]; Zhao and Huang developed numerical models for four full-scale test pavement structures and obtained the stress responses within the subgrade under varying axle loads and wheel wander, proposing recommended axle load equivalence coefficients for different pavement structures [15].

However, several key issues should be recognized. On one hand, previous studies adopting the Apbi

*Address correspondence to this author at the School of Civil Engineering, Southwest Jiaotong University, Chengdu 610031, China; Highway Engineering Key Laboratory of Sichuan Province, Southwest Jiaotong University, Chengdu 610031, China and MOE Key Laboratory of High-speed Railway Engineering, Southwest Jiaotong University, Chengdu 610031, China;
E-mail: xjiang01@163.com

Received on 03-06-2026 Accepted on 07-07-2026 Published on 09-07-2026

E-ISSN: 3083-3590/26

program are all application-oriented research [13-15], which apply this program to calculate mechanical responses under specific engineering conditions rather than verifying and evaluating the program's inherent calculation performance. Most of these studies only focus on vertical load conditions without involving horizontal loads. Xue *et al*. conducted a case study on the internal mechanical response of pavement structures under combined one horizontal load and one vertical load, yet their discussion on horizontal loads remains insufficient [12]. For cases involving one or more horizontal loads, due to the developer not releasing the complete source code and the absence of a comprehensive user manual, clear input specification guidance is lacking, and no systematic reliability assessment of its computational results has been conducted. Consequently, users cannot fully understand the underlying computational principles or verify the accuracy of the outputs, which limits its application scope and the realization of its engineering value. On the other hand, in real service conditions, significant horizontal forces are generated by vehicle starting, braking, acceleration and deceleration. Such loads have a non-negligible influence on pavement damage. Field measurements and research indicate that horizontal forces are not secondary factors, but key load components that jointly govern pavement mechanical responses together with vertical loads [16], and exert a vital influence on the service life of pavement structures. Especially during braking, accelerating or cornering, significant longitudinal or lateral accelerations will inevitably produce larger horizontal loads, which are significantly higher than those under normal driving conditions [17]. These loads can induce significant shear stresses within asphalt layers, which are the primary cause of rutting and top-down shear cracking [18]. When acting on weakly bonded interlayers, they may also cause interlayer slippage and bond failure [19]. At curves or intersections, longitudinal and lateral horizontal forces often coexist, forming a complex bidirectional coupled stress state [20].

Macroscopically, the influence of horizontal loads on asphalt pavement structures is significant. The Apbi program also claims to support horizontal load analysis; however, regrettably, no in-depth studies on its horizontal load input rules and computational reliability have been reported to date. Accordingly, this study aims to systematically investigate issues related to the application of Apbi for asphalt pavement structural analysis under horizontal loading. Specifically, multiple load combination schemes are designed to explore the input rules of Apbi under different horizontal loading conditions; the stress computation results obtained from Apbi are verified by comparison with those from the validated GAMES program; and a practical approximate method is proposed for analyses involving only horizontal loads, while it is demonstrated that Apbi yields erroneous results for the two in-plane shear stress components on the loaded pavement surface.

2. BASIC FORMAT OF LOAD INPUT AND LOADING SCENARIOS IN APBI

According to the limited available documentation, load-related parameters in the Apbi program are specified in the third card group of the input file. The first line contains the number of vertical loads and the number of horizontal loads, separated by an English comma ",". Subsequent lines define the load details: if no horizontal loads are present, each line corresponds to one vertical circular load and lists, in order, the contact pressure (MPa), equivalent circle radius (cm), x-coordinate of the circle center (cm), and y-coordinate of the circle center (cm). All parameters within a line are separated by English commas ",". The coordinate origin must be located at the pavement surface, though its planar position may be arbitrarily defined by the user, and the number of lines equals the number of vertical loads. If horizontal loads are included, after all vertical load parameters have been entered, additional lines are added—one for each horizontal load—specifying the pressure magnitude (MPa) and the angle (°) measured from the positive *x*-axis. The number of these lines equals the number of horizontal loads, and the angle is positive in the direction from the *x*-axis to the *y*-axis.

By employing an enumeration approach, six representative typical loading scenarios were identified under the presence of horizontal loads. These six scenarios comprehensively encompass all possible combinations of vertical and horizontal loads, specifically: (1) horizontal loads only; (2) one vertical load combined with one horizontal load; (3) one vertical load combined with two or more horizontal loads; (4) two or more vertical loads combined with one horizontal load; (5) two or more vertical loads, with the number of horizontal loads being at least two but not exceeding that of vertical loads; and (6) two or more vertical loads, with the number of horizontal loads exceeding that of vertical loads. Descriptions and schematic illustrations of these six typical scenarios are provided in Figure **1**.

It is evident that the Apbi program can accommodate a variety of horizontal load conditions; however, regrettably, existing technical documentation on Apbi usage provides insufficient clarification on how horizontal loads are actually treated in the analysis, which undoubtedly introduces significant uncertainty in its application.

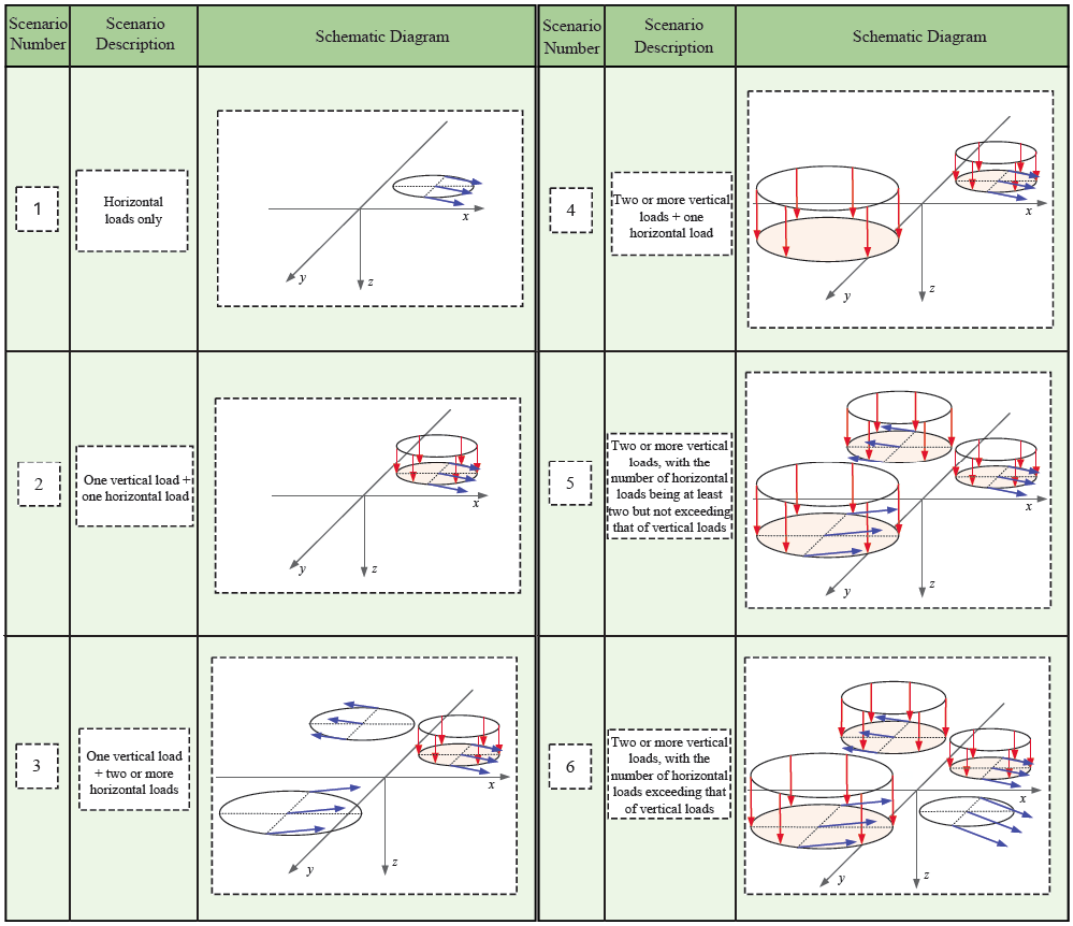

Figure 1: Descriptions and schematic diagrams of six typical loading scenarios.

3. HORIZONTAL LOAD INPUT AND MECHANICAL RESPONSE OF PAVEMENT STRUCTURES WITH APBI

3.1. Numerical Example

Through the above six loading scenarios, the data input and output results of the Apbi program when horizontal loads are considered can be comprehensively examined. In addition, another computer program, GAMES, which is based on the theory of elastic layered systems, is introduced to conduct a comparative and validation study of the mechanical response results obtained from Apbi.

For the purpose of quantitative evaluation, the five-layer elastic system structure is adopted as a numerical example to discuss the various loading scenarios [21]. This five-layer elastic system is shown in Figure **2**, and the parameters of each layer, including the thickness h, elastic modulus E, and Poisson's ratio v, are all provided in Figure **2**. All interlayer interfaces are assumed to be fully continuous.

3.2. Input and Output Presentation of Horizontal Loads under each Loading Scenario

To systematically summarize the performance of the Apbi program under the above six typical loading scenarios, Table **1** lists the specific load parameters for the five-layer elastic system shown in Figure **2**. In Table **1**, δ denotes the radius of the circular load area, x and y are the coordinates of the center of the circular load, and φ is the angle between the horizontal load

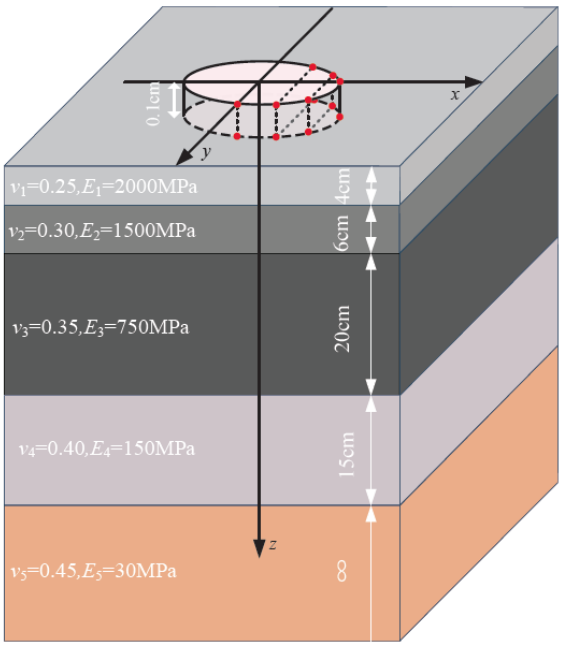

Figure 2: Five-layer elastic system structure (illustrative only; not drawn to scale).

Table 1: Load Parameters for Six Specific Loading Scenarios

Loading scenario	Load type	Load intensity /MPa	δ/cm	(x,y)/cm		φ/°
1	Vertical load	0	10	0	0	
	Horizontal load	1	10	0	0	40
2	Vertical load	2	10	0	0	
	Horizontal load	1	10	0	0	40
3	Vertical load	2	10	0	0	
	Horizontal load	1	10	0	0	40
		1	20	30	0	20
4	Vertical load	2	10	0	0	
		1	20	30	0	
	Horizontal load	1	10	0	0	40
5	Vertical load	2	10	0	0	
		1	20	30	0	
	Horizontal load	1	10	0	0	40
		1	20	30	0	20
6	Vertical load	2	10	0	0	
		1	20	30	0	
	Horizontal load	1	10	0	0	40
		1	20	30	0	20
		1	10	25	0	20

and the x-axis of the global Cartesian coordinate system (the same applies hereafter).

According to Table **1**, the schematic illustrations of the six specific loading scenarios, the load sections of the Apbi input files (i.e., Apbidat files), and the load reproduction sections of the output files (i.e., apbiout files) are presented in Figure **3**.

As shown in Figure **3**:

For loading scenario 1: The output file displays "SYSTEM SKIPPED NO LOADS," indicating that the Apbi program terminated without performing any calculations. This indicates that Apbi cannot currently handle cases involving only horizontal loads directly, and alternative approaches are required to address this issue, as detailed in Section 3.1.

For loading scenario 2: The radius and circle center coordinates of the horizontal load were not input; the program automatically sets them to match those of the corresponding vertical load. It was also observed that the output file converts the angle between the horizontal load and the x-axis of the global Cartesian coordinate system from degrees to radians during data processing. Furthermore, additional examination shows that even if the user inputs different radius and circle center coordinates for the horizontal load, Apbi will forcibly override them to be identical to those of the vertical load and proceed with the calculation. That is, Apbi can only consider cases in which the radius and circle center coordinates of the horizontal and vertical loads are identical.

For loading scenario 4: When there are at least two vertical loads and only one horizontal load, the radius and circle center coordinates of the horizontal load are automatically matched to those of the first vertical load.

For loading scenario 5: The radius and circle center coordinates of the horizontal and vertical loads exhibit a strict one-to-one correspondence.

For loading scenarios 3 and 6: When the number of horizontal loads exceeds that of vertical loads, the excess horizontal loads have their radii automatically set to zero, meaning that they do not participate in the calculation. The resulting mechanical response is identical to the case where the number of horizontal and vertical loads is equal. Notably, the program provides no warning or prompt for this behavior, in stark contrast to the clear message "SYSTEM SKIPPED NO LOADS" issued when only horizontal loads are applied.

3.3. Stress Calculation Results Analysis and Discussion

3.3.1. Reliability Verification of Horizontal Load Consideration in the GAMES Program

Since another computer program, GAMES, which is also based on the theory of elastic layered systems, is subsequently adopted as a benchmark to examine the correctness of Apbi in considering horizontal loads, the

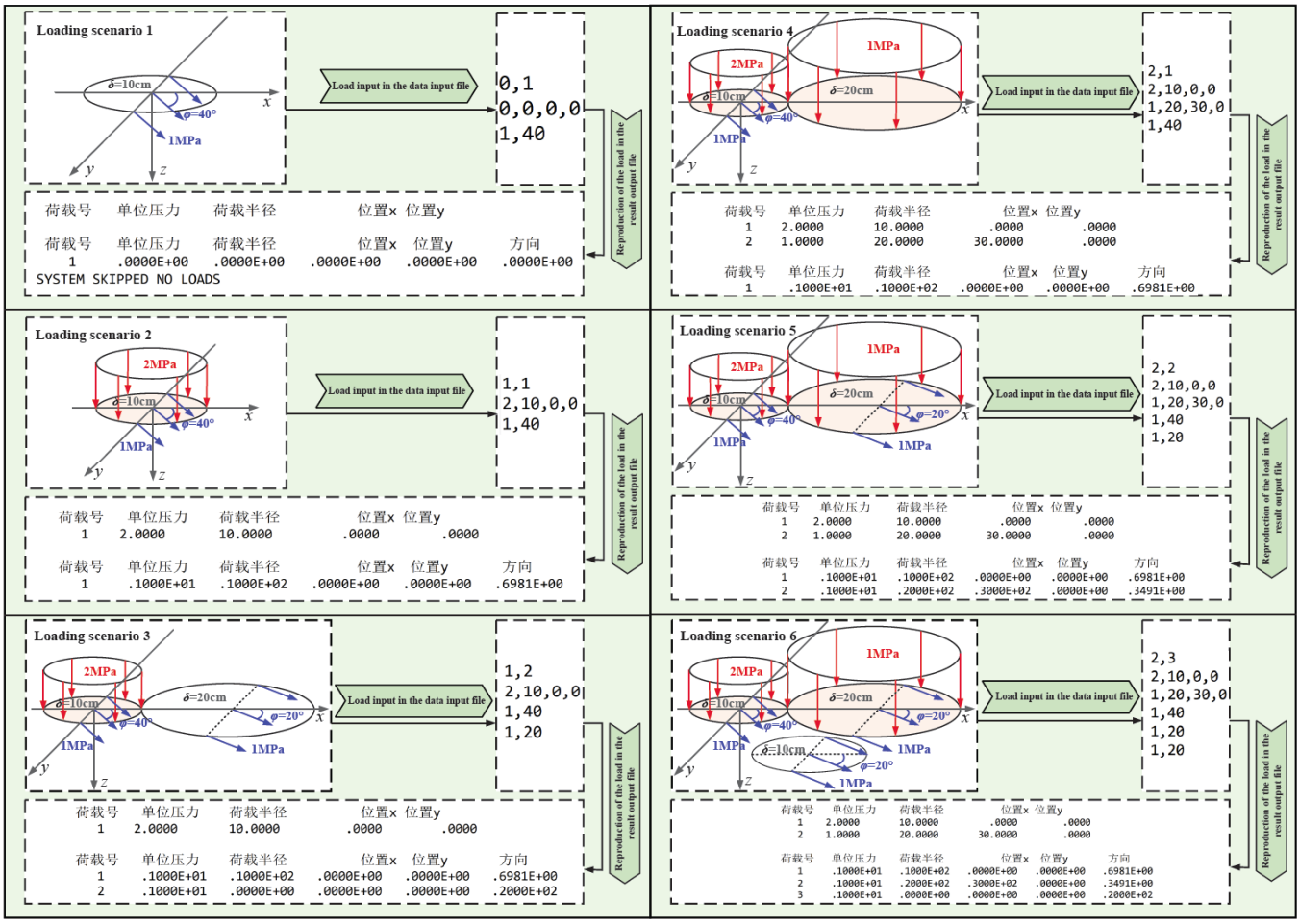

Figure 3: Input and output of loads under each loading scenario.

(Note: Screenshot from Chinese-language Apbi interface; key terms: 荷载号 = Load ID, 单位压力 = Unit pressure, 荷载半径 = Load radius, 位置x/y = x/y-position, 方向 = Direction.)

numerical example from Wang is adopted to verify the reliability of the results obtained from GAMES when horizontal loads are taken into account [21]. The model consists of a five-layer elastic system (Figure **2**) subjected to a single uniformly distributed circular horizontal load, with a load intensity of p=1MPa, a load radius of δ=10cm, and the circle center of the loading area located at the origin (0,0). The angle φ=40° is defined between the horizontal load direction and the positive x-axis of the global Cartesian coordinate system. Six calculation points are all located on the surface of the first layer (z=0 cm) along a circle with a radius of r=5 cm, and their planar locations are shown in Figure **4**.

Following the calculations, Table **2** presents the stress results at the six calculation points obtained from the GAMES program in the Cartesian coordinate system.

It should be noted that the stress components listed in Table **2** are all expressed in the Cartesian coordinate system, whereas Wang reported stress components in the cylindrical coordinate system based on their self-developed NESCP program [21]. Therefore, a

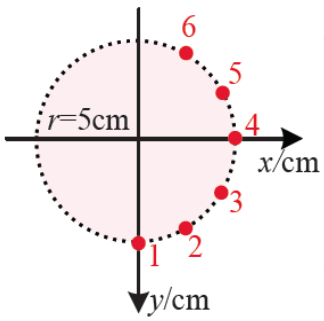

Point ID	x/cm	y/cm
1	0	5
2	2.5	4.33
3	4.33	2.5
4	5	0
5	4.33	-2.5
6	2.5	-4.33

Figure 4: Planar locations of the calculation points.

Table 2: Stress Results from the GAMES Program Under Horizontal Load only (Unit: MPa)

Point ID	σ_x	σ_y	σ_z	τ_{yz}	τ_{xz}	τ_{xy}
1	-0.08360	-0.46360	0.00000	-0.64279	-0.76605	-0.22705
2	-0.34888	-0.45105	0.00000	-0.64279	-0.76605	-0.29123
3	-0.52013	-0.31820	0.00000	-0.64279	-0.76605	-0.27782
4	-0.55249	-0.09963	0.00000	-0.64279	-0.76605	-0.19052
5	-0.43732	0.14618	0.00000	-0.64279	-0.76605	-0.05170
6	-0.20454	0.35235	0.00000	-0.64279	-0.76605	0.10149

coordinate transformation is required to convert the GAMES results from the Cartesian coordinate system to the cylindrical coordinate system. The transformation equations are as follows, where θ is the angle between calculation point A and the positive x-axis of the global Cartesian coordinate system; x_A, y_A are the x and y coordinates of calculation point A; and x_i , y_i are the coordinates of the load circle center.

$$\theta = \arctan\frac{y_A - y_i}{x_A - x_i} \tag{1}$$

$$\sigma_r = \sigma_x \cos^2\theta + \sigma_y \sin^2\theta + 2\tau_{xy}\cos\theta\cdot\sin\theta \tag{2}$$

$$\sigma_\theta = \sigma_x \sin^2\theta + \sigma_y \cos^2\theta - 2\tau_{xy}\cos\theta\cdot\sin\theta \tag{3}$$

$$\sigma_z = \sigma_z \quad \text{(the axial normal stress remains unchanged)} \tag{4}$$

$$\tau_{r\theta} = (\sigma_y - \sigma_x)\cdot\cos\theta\cdot\sin\theta + \tau_{xy}\cdot(\cos^2\theta - \sin^2\theta) \tag{5}$$

$$\tau_{\theta z} = -\tau_{zx}\sin\theta + \tau_{yz}\cos\theta \tag{6}$$

$$\tau_{zr} = \tau_{zx}\cos\theta + \tau_{yz}\sin\theta \tag{7}$$

It should be particularly emphasized that NESCP is a computer program developed by Wang based on the theory of elastic layered systems, and its reliability has been thoroughly validated [21]. The transformed GAMES results are now compared with those obtained from the NESCP program, as shown in Table **3**. For each point ID, the values without parentheses correspond to the stress results from GAMES, while those in parentheses are from NESCP.

As shown in Table **3**, when the NESCP results are taken as the benchmark, the deviations of the GAMES results from those of NESCP are small and generally negligible. Therefore, the GAMES program can be considered correct and reliable in computing the mechanical response under horizontal loading. Furthermore, since GAMES is also capable of considering uniformly distributed vertical loads, it can be adopted in subsequent analyses as a computational platform that simultaneously accounts for both vertical and horizontal loads, thereby enabling validation of the Apbi program results.

3.3.2. Comparison of Stress Results between Apbi and GAMES

Based on the above analysis, the stress results from Apbi and GAMES at the six calculation points within the first layer (z=0.1 cm) under the typical loading cases defined in Section 3.2 are compared below. The five-layer elastic system and the planar

Table 3: Comparison of Results from GAMES and NESCP (Unit: MPa)

Point ID	σ_r	σ_θ	σ_z	$\tau_{r\theta}$	$\tau_{\theta z}$	τ_{zr}
1	-0.4636	-0.0836	0	0.2271	0.7661	-0.6428
	(-0.4624)	(-0.0833)	(0)	(0.2271)	(0.7660)	(-0.6428)
2	-0.6777	-0.1222	0	0.1014	0.3420	-0.9397
	(-0.6759)	(-0.1218)	(0)	(0.1014)	(0.3420)	(-0.9397)
3	-0.7102	-0.1281	0	-0.0515	-0.1736	-0.9848
	(-0.7084)	(-0.1276)	(0)	(-0.0515)	(-0.1736)	(-0.9848)
4	-0.5525	-0.0996	0	-0.1905	-0.6428	-0.7661
	(-0.5510)	(-0.0993)	(0)	(-0.1905)	(-0.6428)	(-0.7660)
5	-0.2467	-0.0445	0	-0.2785	-0.9397	-0.3420
	(-0.2460)	(-0.0443)	(0)	(-0.2785)	(-0.9397)	(-0.3420)
6	0.1252	0.0226	0	-0.2919	-0.9848	0.1736
	(0.1249)	(0.0225)	(0)	(-0.2919)	(-0.9848)	(0.1736)

Note: NESCP results are cited from Wang [21].

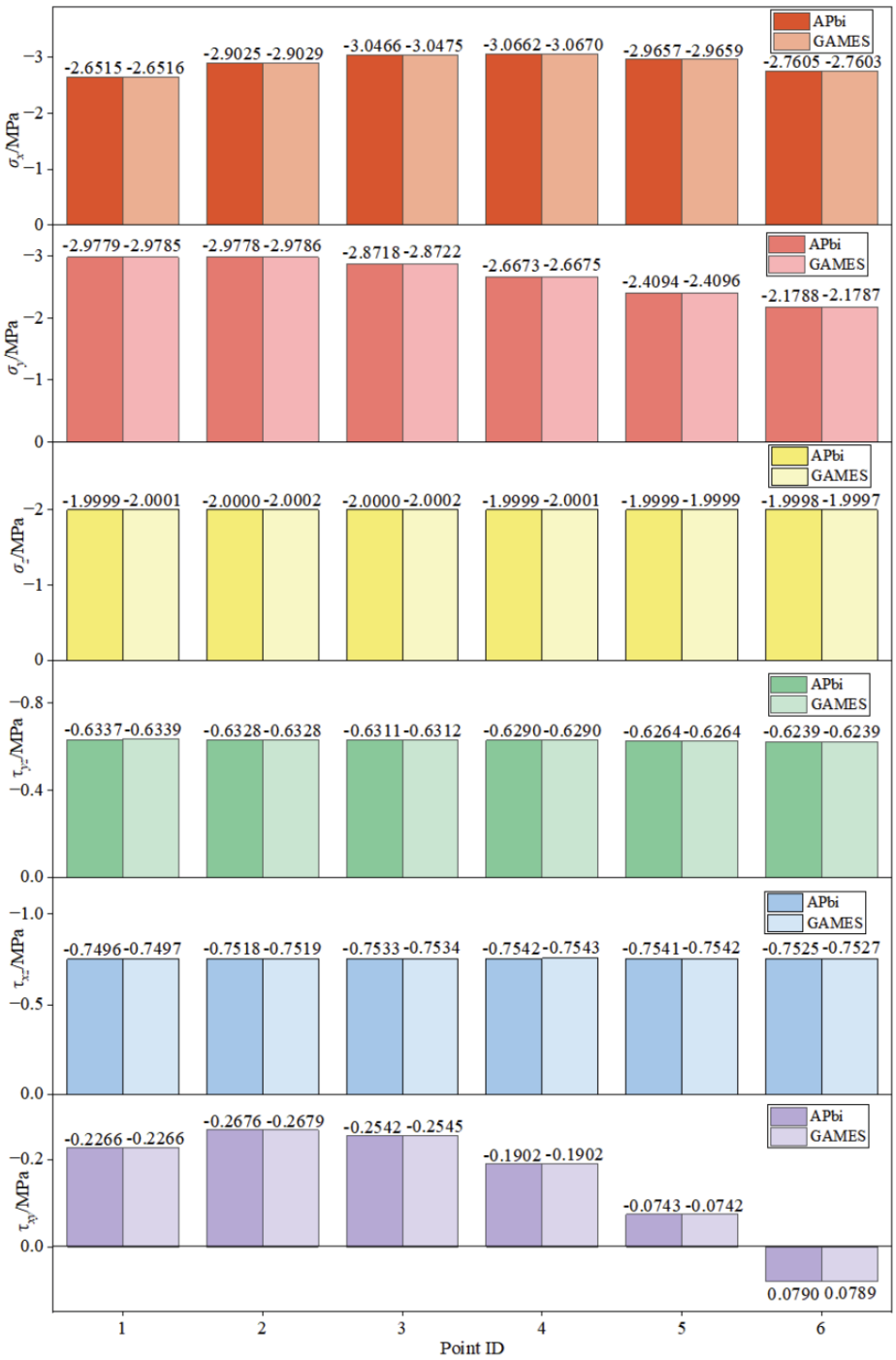

Figure 5: Comparison of results from Apbi and GAMES under Case 2.

locations of the calculation points are identical to those in the numerical example from Wang, with detailed information provided in Figures **2** and **4**, respectively [21]. It should be noted that, as indicated in Section 3.2, the mechanical responses obtained under Case 2 and Case 3, as well as those under Case 5 and Case 6, are respectively identical. Therefore, only the stress results for Case 2, Case 4, and Case 5 are presented, as shown in Figures **5**, **6**, and **7**, respectively.

The results under Case 2, Case 4, and Case 5 indicate that, except for the pure horizontal loading case which yielded a “SYSTEM SKIPPED NO LOADS” message, all other complex loading scenarios involving horizontal loads—identified through enumeration—were computed correctly.

When the stress results from the two programs are in close agreement, it suggests that the Apbi program is accurate and reliable under the corresponding loading condition. The minor discrepancies observed between the two sets of results may be attributed to the following factors: the theory of multilayer elastic systems involves special functions and integral transforms; the two programs may differ in their default settings for parameters such as the allowable tolerance

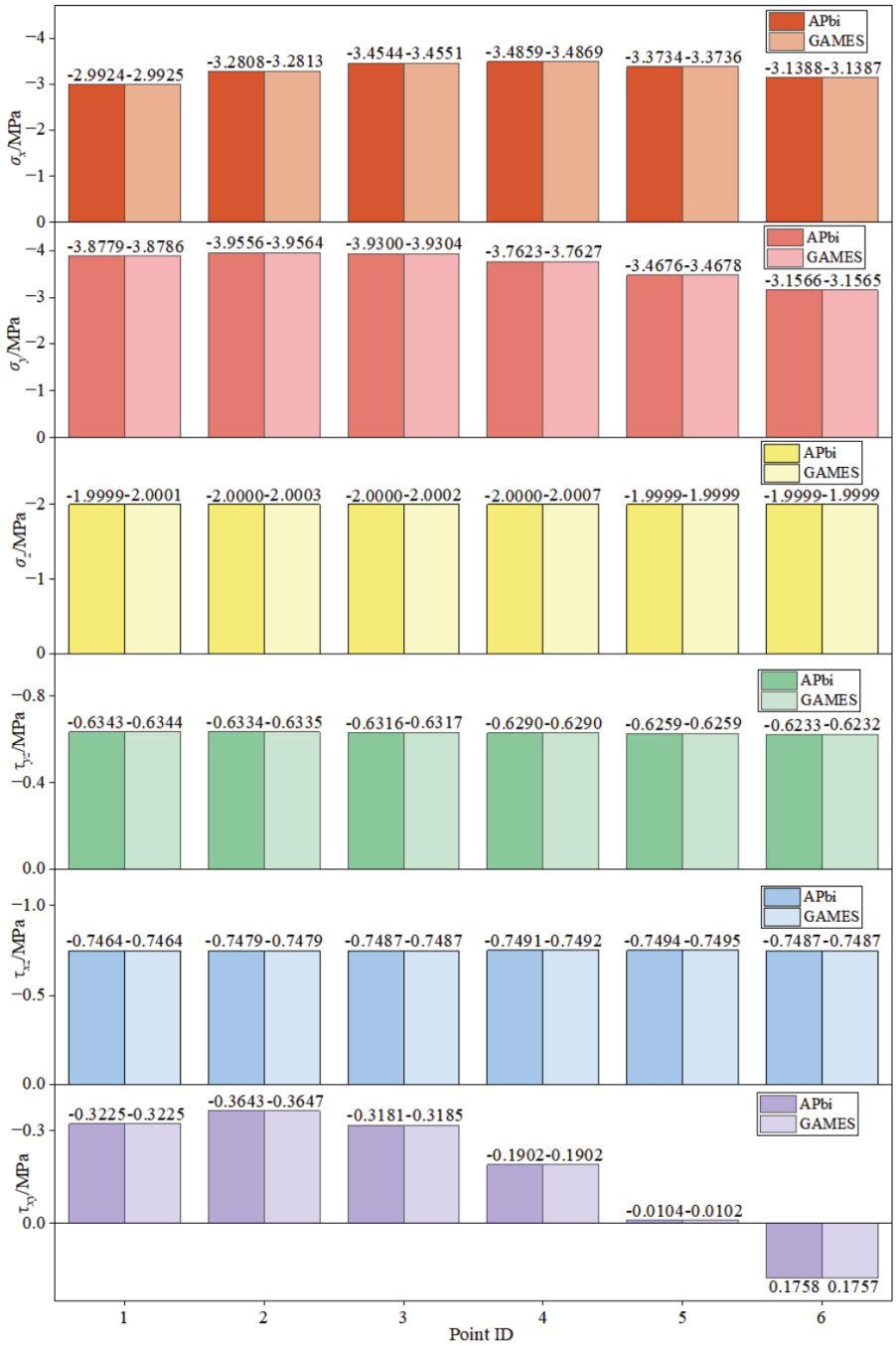

Figure 6: Comparison of results from Apbi and GAMES under Case 4.

in integrals containing Bessel functions and the maximum number of iterations in recursive integration involving Bessel functions [12]. Additionally, Apbi takes load intensity as pressure (MPa) as input, whereas GAMES uses wheel load (kN); rounding errors introduced during unit conversion may also contribute to the differences.

4. FURTHER DISCUSSION

4.1. Approximate Treatment of Purely Horizontal Loading Cases

As indicated in Section 3.2, when only horizontal loads are applied, Apbi outputs the message “SYSTEM SKIPPED NO LOADS.” To address this issue, a very small vertical load (e.g., $q = 10^{-5}$ MPa) can be introduced, with its circle center and radius identical to those of the target horizontal load. Following the previous study [21], a five-layer elastic system is considered, as shown in Figure **2**. A circular uniformly distributed load is applied with a vertical load intensity of $q = 10^{-5}$ MPa, a horizontal load intensity of $p = 1$ MPa, a loading circle radius of $\delta = 10$ cm, and the circle center located at the origin (0, 0). The horizontal load forms an angle of $\varphi = 40°$ with the global x-axis. The calculation points are located within the first layer ($z = 0.1$ cm), with their planar coordinates detailed in Figure **4**. The Apbi output results are presented in Table **4**.

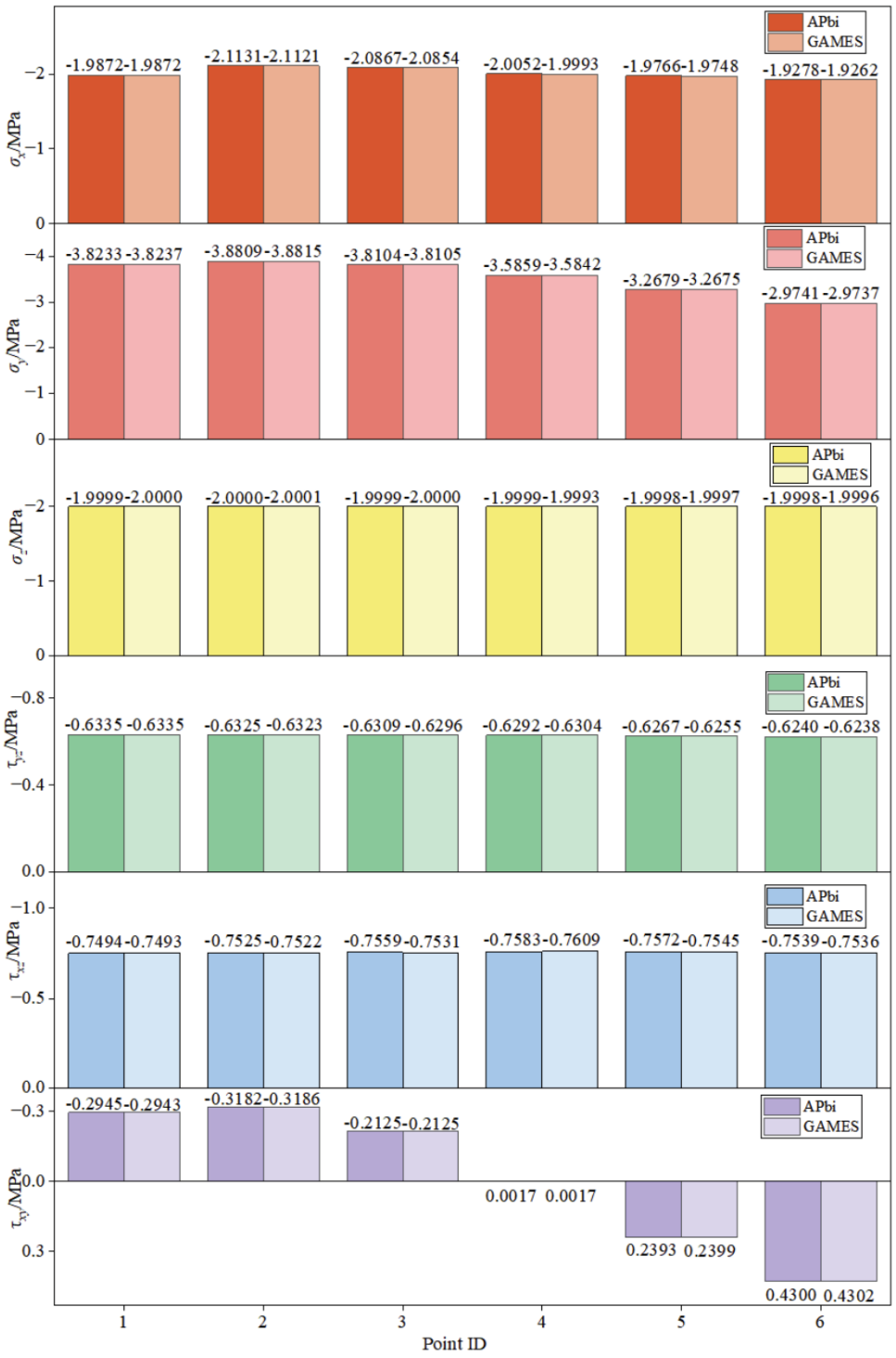

Figure 7: Comparison of results from Apbi and GAMES under Case 5.

Table 4: Apbi Output Results (Unit: MPa)

Point ID	σ_x	σ_y	σ_z	τ_{yz}	τ_{xz}	τ_{xy}
1	-0.0825	-0.4608	-0.0001	-0.6281	-0.7496	-0.2266
2	-0.3465	-0.4477	-0.0001	-0.6278	-0.7489	-0.2900
3	-0.5165	-0.3158	-0.0001	-0.6283	-0.7484	-0.2766
4	-0.5491	-0.0983	-0.0001	-0.6290	-0.7485	-0.1902
5	-0.4356	0.1465	0.0000	-0.6292	-0.7492	-0.0519
6	-0.2045	0.3512	0.0000	-0.6288	-0.7497	0.1014

Table 5: Comparison of Results from Apbi and NESCP (Unit: MPa)

Point ID	σ_r	σ_θ	σ_z	$\tau_{r\theta}$	$\tau_{\theta z}$	τ_{zr}
1	-0.4608	-0.0825	-0.0001	0.2266	0.7496	-0.6281
	(-0.4608)	(-0.0825)	(-0.0001)	(0.2266)	(0.7496)	(-0.6281)
2	-0.6735	-0.1207	-0.0001	0.1012	0.3347	-0.9181
	(-0.6736)	(-0.1206)	(-0.0001)	(0.1012)	(0.3347)	(-0.9182)
3	-0.7059	-0.1264	-0.0001	-0.0514	-0.1699	-0.9623
	(-0.7059)	(-0.1264)	(-0.0001)	(-0.0514)	(-0.1699)	(-0.9623)
4	-0.5491	-0.0983	-0.0001	-0.1902	-0.6290	-0.7485
	(-0.5491)	(-0.0983)	(-0.0001)	(-0.1902)	(-0.6290)	(-0.7485)
5	-0.2451	-0.0440	0.0000	-0.2780	-0.9195	-0.3342
	(-0.2452)	(-0.0439)	(0.0000)	(-0.2780)	(-0.9195)	(-0.3342)
6	0.1245	0.0222	0.0000	-0.2913	-0.9637	0.1697
	(0.1245)	(0.0223)	(0.0000)	(-0.2913)	(-0.9637)	(0.1697)

Note: NESCP results are cited from Wang [21].

The Apbi results, transformed from the Cartesian to the cylindrical coordinate system using the formulas provided in Section 3.3.1, are compared with the reference results computed using the NESCP program [21], as presented in Table **5**. For the same calculation point, values without parentheses correspond to the Apbi results, while those in parentheses correspond to the NESCP results.

The results in Table **5** indicate that, after introducing a negligible vertical load (q = 10^{-5} MPa), Apbi and NESCP results are in close agreement. This demonstrates that, through such an approximation, Apbi can be used to analyze cases with only horizontal loads. Further trials show that, when the number of horizontal loads exceeds that of vertical loads, negligible vertical loads—equal in number to the excess horizontal loads—can be introduced, provided that their radii and centers exactly match those of the corresponding horizontal loads. Under this condition, the excess horizontal loads participate normally in the computation, rather than being excluded as in Section 3.2 where their radii were effectively set to zero.

To quantitatively evaluate this approximate method, scatter plots are employed (Figure **8**). The horizontal axis represents σ_x at six calculation points under four vertical load levels (10^{-1}, 10^{-2}, 10^{-3}, and 10^{-4} MPa); the vertical axis uses σ_x at the same points under q = 10^{-5} MPa as the benchmark. This case is adopted as the benchmark because its results match exact NESCP solutions with high consistency, thereby representing the true stress state under pure horizontal loading while avoiding repeated coordinate transformations between Cartesian and cylindrical systems. The dashed line y = x serves as the zero-error reference; deviation from this baseline indicates the error magnitude of the approximate method.

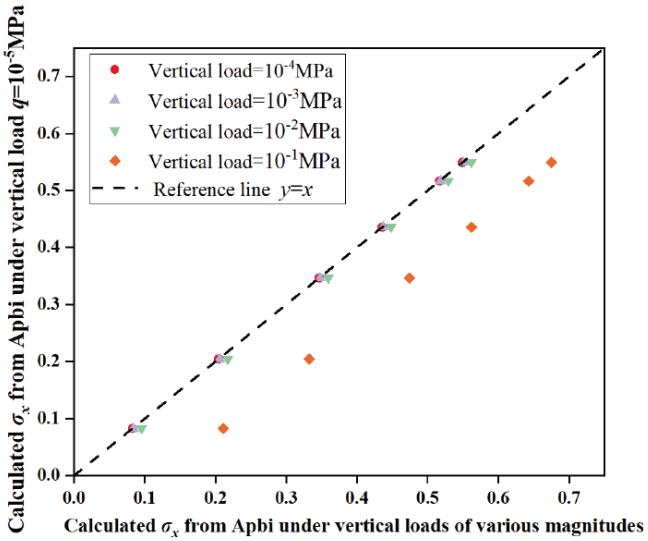

Figure 8: Effect of vertical load magnitude on the σ_x calculation accuracy at six calculation points.

As shown in Figure **8**, under the previously specified condition of a horizontal load of 1 MPa, all scatter points closely align with the reference line y = x when the vertical-to-horizontal load ratio satisfies q/p < 10^{-3}, indicating that the approximate method meets engineering accuracy requirements. When this ratio increases to q/p = 10^{-2}, and the scatter points deviate significantly, the calculation error becomes non-negligible, and the approximation is no longer valid. For practical engineering applications, provided that the numerical program converges properly, an extremely small vertical load (e.g., 10^{-5} MPa) should be adopted to minimize interference from the introduced vertical load and ensure the accuracy of the equivalent results.

4.2. Incorrect in-Plane Shear Stress Components on the Pavement Surface

Wang points out that the internationally recognized BISAR 2.0 program contains a clear error in its source code: when computing the stress components at surface points (z=0 cm) located within the loading circle ($r \leqslant \delta$) under a circular uniformly distributed horizontal load, the radial stress $\tau_{\theta z}$ and the shear stress τ_{zr} are incorrect [21]. Whether the Apbi program exhibits the same potential error remains unknown, and this issue is examined in detail below.

The numerical example from Section 4.1 is again employed, with the calculation points adjusted to the surface of the first layer (z=0 cm). The configuration of the five-layer elastic system and the planar coordinates of the calculation points are shown in Figures **2** and **4**, respectively. Following the treatment described in Section 4.1, a very small vertical load (q=10^{-5} MPa) is introduced. The Apbi results are presented in Table **6**.

The Apbi results are transformed from the Cartesian to the cylindrical coordinate system using the formulation described in Section 3.3.1, and then compared with the reference results from the BISAR 2.0 and NESCP programs obtained by Wang, as presented in Table **7** [21]. The first row shows the Apbi results, while the second row presents the BISAR 2.0 results in parentheses. Note that the BISAR 2.0 program exhibits errors only in the $\tau_{\theta z}$ and τ_{zr} components; all other stress components are identical to those of NESCP. For $\tau_{\theta z}$ and τ_{zr}, the values to the right correspond to the NESCP results.

Inspection of Table **7** clearly shows that the $\tau_{\theta z}$ and τ_{zr} components of the Apbi results, after conversion to the cylindrical coordinate system, are nearly identical to the erroneous results from BISAR 2.0, and significantly different from the reference solutions. It is particularly noteworthy that, for pairs of calculation points sharing the same x and y coordinates but with z=0 cm and z=0.1 cm, respectively, the computed stress components σ_r, σ_θ, σ_z, and $\tau_{r\theta}$ are all relatively close due to the proximity of their spatial positions under the horizontal load. However, the two shear components $\tau_{\theta z}$ and τ_{zr} exhibit anomalous behavior. This indicates that the Apbi program contains an error similar to that in BISAR 2.0: when analyzing a layered elastic system

Table 6: Apbi Calculation Results (Unit: MPa)

Point ID	σ_x	σ_y	σ_z	τ_{yz}	τ_{xz}	τ_{xy}
1	-0.0833	-0.4624	0.0000	-0.7660	-0.6428	-0.2271
2	-0.3481	-0.4496	0.0000	-0.3420	-0.9397	-0.2906
3	-0.5186	-0.3174	0.0000	0.1736	-0.9848	-0.2772
4	-0.5510	-0.0993	0.0000	0.6428	-0.7660	-0.1905
5	-0.4368	0.1465	0.0000	0.9397	-0.3420	-0.0519
6	-0.2047	0.3521	0.0000	0.9848	0.1736	0.1016

Table 7: Comparison of Results from Apbi, BISAR 2.0, and NESCP (Unit: MPa)

Point ID	σ_r	σ_θ	σ_z	$\tau_{r\theta}$	$\tau_{\theta z}$		τ_{zr}	
1	-0.4624	-0.0833	0.0000	0.2271	0.6428	0.7660	-0.7660	-0.6428
	(-0.4624)	(-0.0833)	(0.0000)	(0.2271)	(0.6428)		(-0.7660)	
2	-0.6759	-0.1218	0.0000	0.1013	0.6428	0.3420	-0.7660	-0.9397
	(-0.6759)	(-0.1218)	(0.0000)	(0.1014)	(0.6428)		(-0.7660)	
3	-0.7084	-0.1276	0.0000	-0.0515	0.6427	-0.1736	-0.7661	-0.9848
	(-0.7084)	(-0.1276)	(0.0000)	(-0.0515)	(0.6428)		(-0.7660)	
4	-0.5491	-0.0993	0.0000	-0.1905	0.6428	-0.6428	-0.7660	-0.766
	(-0.5510)	(-0.0993)	(0.0000)	(-0.1905)	(0.6428)		(-0.7660)	
5	-0.2460	-0.0443	0.0000	-0.2785	0.6428	-0.9397	-0.7660	-0.342
	(-0.2460)	(-0.0443)	(0.0000)	(-0.2785)	(0.6428)		(-0.7660)	
6	0.1249	0.0225	0.0000	-0.2919	0.6427	-0.9848	-0.7661	0.1736
	(0.1249)	(0.0225)	(0.0000)	(-0.2919)	(0.6428)		(-0.7660)	

Note: The results from BISAR 2.0 and NESCP are cited from Wang [21].

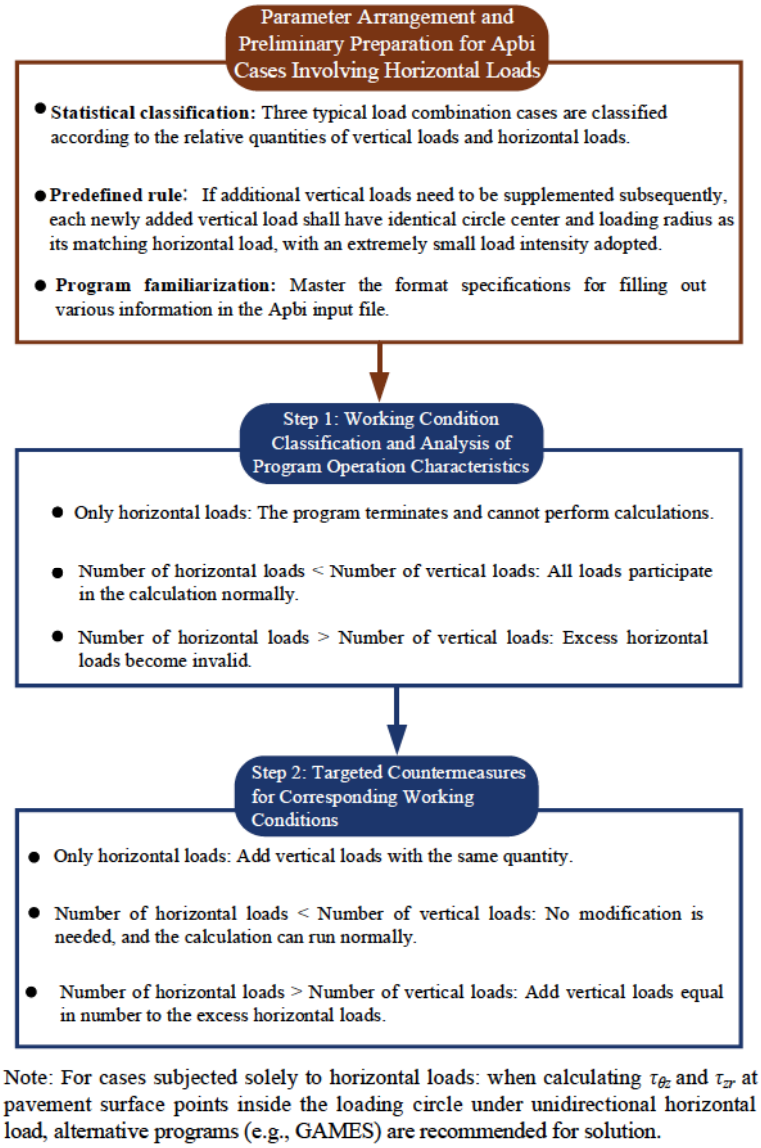

Figure 9: Full Flowchart for Processing Combined Load Cases with Horizontal Loads Using Apbi.

subjected to a circular uniformly distributed unidirectional horizontal load, the computed $\tau_{\theta z}$ and τ_{zr} components at surface points (z=0 cm) located within the loaded area ($r \leqslant \delta$, where r is the radial coordinate of the calculation point and δ is the radius of the loading circle) are incorrect.

The aforementioned error in shear stress calculation undoubtedly exerts a non-negligible impact on pavement structural design and the interpretation of pavement distress mechanisms. In structural design, shear stresses near the pavement surface within the loaded region are frequently examined to conduct shear resistance verification for pavement structures; meanwhile, the initiation and propagation of top-down cracks are governed by surface shear stresses. Accordingly, if the calculated $\tau_{\theta z}$ and τ_{zr} values for calculation points on the pavement surface inside the loaded circle ($r \leqslant \delta$) are unreliable, the aforementioned analyses cannot be performed correctly.

To further assist users in properly applying the Apbi program for analyzing asphalt pavement structures under horizontal loads, this study summarizes the complete implementation procedure of Apbi for cases involving horizontal loads, as illustrated in Figure **9**.

5. CONCLUSIONS AND RECOMMENDATIONS

Using the enumeration method, six representative typical loading cases involving horizontal loads were summarized, and the precautions for horizontal load input under each case were clarified; the stress calculation results for all cases agree well with those from the GAMES program. This study finds that when the number of horizontal loads exceeds that of vertical loads in Apbi, the radius of the excess horizontal loads is set to zero, and such loads are effectively excluded from computation. For cases with only horizontal loads, one may introduce an equal number of vertical loads with negligibly small intensity, whose radii and centers must exactly correspond to those of the target

horizontal loads; similarly, when horizontal loads outnumber vertical loads, this strategy can be applied to ensure the excess horizontal loads participate in the calculation. Moreover, analogous to BISAR 2.0, Apbi yields incorrect values for the two shear stress components at surface points of the layered elastic system located within the loaded circular area under unidirectional horizontal loading.

Based on the above findings, two practical suggestions are proposed:

(1) For direct application, since Apbi produces erroneous results for the two surface shear stress components within the loaded circle, alternative programs such as GAMES are recommended for reliable computation;

(2) For future program enhancement, it is advisable to implement a pop-up warning when the number of horizontal loads exceeds that of vertical loads, informing users that some loads are not included in the calculation—or alternatively, to revise and expand the official user manual to explicitly document this behavior.

FUNDING

The research was supported by National Natural Science Foundation of China (52578533).

CONFLICTS OF INTEREST

The authors declare that they have no conflict of interest.

AVAILABILITY OF DATA AND MATERIAL

Data will be made available on request.

CODE AVAILABILITY

Not applicable.

AUTHORS' CONTRIBUTIONS

Yipeng Chen: Software, Data curation, Writing – original draft. Xin Jiang: Supervision, Conceptualization, Methodology. Yangchen Lu: Software, Investigation. Xinya Huang: Software, Investigation. Canyang Cui: Writing – review & editing. Yang Xue: Software, Investigation. Shixuan Li: Software, Investigation. Hongpo Liu: Writing – review & editing. Yanjun Qiu: Investigation.

ETHICS APPROVAL AND CONSENT TO PARTICIPATE

We hereby confirm that all necessary ethics approval and informed consent have been obtained for the research conducted, in accordance with institutional and ethical guidelines.

CONSENT FOR PUBLICATION

We hereby confirm that we have obtained the necessary consent for publication from all relevant parties involved in this work, and we declare that we have the right to publish this material.

REFERENCES

[1] Huang Y H. Pavement analysis and design[M]. Upper Saddle River, NJ: Pearson/Prentice Hall, 2004.

[2] Cui C, Jiang X, Sun R, *et al.* Fatigue characteristics of cement-stabilized steel slag base course for asphalt pavement structure considering different paving methods. International Journal of Pavement Engineering 2024; 25(1): 2393313. https://doi.org/10.1080/10298436.2024.2393313

[3] Li Z, Jiang X, Liu H, *et al.* Assessment on asphalt pavement nonlinear analysis techniques of Everstress computer program. International Journal of Pavement Research and Technology 2025: 1-16. https://doi.org/10.1007/s42947-025-00634-0

[4] Jiang X, Yao K, Gu H, *et al.* Comparison of nonlinear analysis algorithms for two typical asphalt pavement analysis programs. The Baltic Journal of Road and Bridge Engineering 2020; 15(4): 225-251. https://doi.org/10.7250/bjrbe.2020-15.502

[5] Zhang M, Jiang X, Qiu Y. Influence of nonlinear analysis technology on damage analysis of asphalt pavement structure. The Baltic Journal of Road and Bridge Engineering 2023; 18(3): 1-26. https://doi.org/10.7250/bjrbe.2023-18.606

[6] Mamlouk M, Zaniewski J, He W. Analysis and design optimization of flexible pavement. Journal of Transportation Engineering 2000; 126(2): 161-167. https://doi.org/10.1061/(ASCE)0733-947X(2000)126:2(161)

[7] Babiker L, Jiang X, Zhang M, *et al.* Comparisons of asphalt pavement structure interlayer bonding algorithms for typical computer programs. International Journal of Pavement Research and Technology 2025: 1-19. https://doi.org/10.1007/s42947-025-00663-9

[8] Putri E, Liew S, Mannan M, *et al.* StormPav pavement using different wheel loads. GEOMATE Journal 2022; 22(89): 1-8. https://doi.org/10.21660/2022.89.j2354

[9] Tutu K, Timm D. Recursive pseudo fatigue cracking damage model for asphalt pavements. International Journal of Pavement Engineering 2022; 23(8): 2654-2674. https://doi.org/10.1080/10298436.2020.1867856

[10] Dalla Valle P, Thom N. Improvement to method of equivalent thicknesses (MET) for calculation of critical strains for flexible pavements. International Journal of Pavement Engineering 2018; 19(12): 1053-1060. https://doi.org/10.1080/10298436.2016.1238698

[11] Zhang M, Jiang X, Liu H, *et al.* Development optimization of computer programs for asphalt pavement structure based on Burmister's layered theory from application perspective. International Journal of Pavement Research and Technology 2025; 18(6): 1412-1427. https://doi.org/10.1007/s42947-024-00423-1

[12] Xue Y, Jiang X, Liu H, *et al.* Assessment of Apbi computer program developed by multi-layer elastic system theory. Transportation Science & Technology 2025; (4): 7-13.

[13] Chen F, Huang X. Analysis of the mechanical response of rigid base asphalt pavement under heavy load. Journal of Highway and Transportation Research and Development 2007; (6): 41-45.

[14] Huang X, Gao J. Sensitivity analysis of pavement structures under heavy traffic load. Journal of Highway and Transportation Research and Development 2004; (12): 1-4.

[15] Zhao R, Huang X. Vehicle axle load conversion based on stress parameters of asphalt road soil foundation. Journal of Highway and Transportation Research and Development 2020; 37(7): 9-16.

[16] Yan G, Ye Z, Wang W, *et al.* Numerical analysis on distribution and response of acceleration field of pavement under moving load. International Journal of Pavement Research and Technology 2021; 14(5): 519-529. https://doi.org/10.1007/s42947-020-0179-9

[17] Li L, Gan J, Ji X, *et al.* Dynamic driving risk potential field model under the connected and automated vehicles environment and its application in car-following modeling. IEEE Transactions on Intelligent Transportation Systems 2022; 23(1): 122-141. https://doi.org/10.1109/TITS.2020.3008284

[18] Norouzi A, Kim D, Richard Kim Y. Numerical evaluation of pavement design parameters for the fatigue cracking and rutting performance of asphalt pavements. Materials and Structures 2016; 49(9): 3619-3634. https://doi.org/10.1617/s11527-015-0744-x

[19] Yang Z, Huang W, Wang J, *et al.* Investigation of interlayer bonding performance between cement concrete pavements and asphalt ultra-thin overlays. Construction and Building Materials 2025; 486: 141965. https://doi.org/10.1016/j.conbuildmat.2025.141965

[20] Cordeiro R, Victorino A, Azinheira J, *et al.* Estimation of vertical, lateral, and longitudinal tire forces in four-wheel vehicles using a delayed interconnected cascade-observer structure. IEEE/ASME Transactions on Mechatronics 2019; 24(2): 561-571. https://doi.org/10.1109/TMECH.2019.2899261

[21] Wang K. The latest research progress of mechanics of layered elastic system—on an obvious error in BISAR source program. Mechanics in Engineering 2025; 47(1): 189-194.

https://doi.org/10.65904/3083-3590.2026.02.04